



# Efficient SAV approach for imaginary time gradient flows with applications to one- and multi-component Bose-Einstein Condensates



Qingqu Zhuang<sup>a,1</sup>, Jie Shen<sup>b,\*,2</sup>

<sup>a</sup> Fujian Province University Key Laboratory of Computational Science, School of Mathematical Sciences, Huaqiao University, Quanzhou 362021, China

<sup>b</sup> Department of Mathematics, Purdue University, West Lafayette, IN 47907, USA

## ARTICLE INFO

### Article history:

Received 22 February 2019

Received in revised form 27 May 2019

Accepted 17 June 2019

Available online 27 June 2019

### Keywords:

SAV approach

Imaginary time gradient flow

Ground state

Bose-Einstein Condensates

## ABSTRACT

Efficient and accurate numerical schemes, based on the scalar auxiliary variable (SAV) approach, are proposed to find the ground state solutions of one- and multi-component Bose-Einstein Condensates (BECs). Two types of SAV schemes are proposed: the first is based on the original SAV scheme for the imaginary time gradient flow of BECs which is accurate for the dynamic evolution; the second is a modified SAV scheme based on the normalized imaginary time gradient flow and leads to fast convergence towards the steady state solutions. Detailed numerical comparison with existing methods based on projection to the constrained space indicates that the modified SAV schemes are more efficient, particularly for the multi-component BECs.

© 2019 Elsevier Inc. All rights reserved.

## 1. Introduction

The Bose-Einstein condensation (BEC) has attracted vast interests and has been extensively studied since its first experimental realization [2]. Numerous numerical methods are developed to compute their ground state solutions which are minimizers of the free energy of the BEC system, including Runge–Kutta spectral method [16], Gauss–Seidel-type methods [11], finite element method by directly minimizing the energy functional [10], regularized Newton method [23], preconditioned nonlinear conjugate gradient method [3], the normalized imaginary time gradient flow method [5,8,13], and normalized imaginary time gradient flow method with attractive–repulsive splitting [17]. In particular, the methods based on a normalized imaginary time gradient flow have been very popular thanks to its simplicity and efficiency. It is observed in [8] that the most efficient scheme based on normalized imaginary time gradient flow is the linearized backward–Euler scheme with a projection to enforce the norm conservation. While the projection step is simple to implement in the one-component case, it becomes much more complicated for multi-component BECs [5,7]. So there is a need to find an alternative method to deal with multi-component BECs.

\* Corresponding author.

E-mail addresses: qqzhuang@hqu.edu.cn (Q. Zhuang), shen7@purdue.edu (J. Shen).

<sup>1</sup> The work of this author is supported by the National Natural Science Foundation of China (Nos. 11501224, 11771083), and the Promotion Program for Young and Middle-aged Teacher in Science and Technology Research of Huaqiao University (No. ZQN-PY201).

<sup>2</sup> The work of J.S. is partially supported by NSF grants DMS-1620262 and DMS-1720442, and AFOSR FA9550-16-1-0102.

Recently, an interesting method, the so called scalar auxiliary variable (SAV) approach, is proposed for solving a large class of gradient flows (cf. [19–21]). The method has several distinct advantages over other approaches so it is natural to apply the SAV approach to the imaginary time gradient flow for computing ground state solutions for BECs. However, several issues arise: (i) the SAV approach does not have a mechanism to enforce additional constraints imposed on the gradient flow; (ii) the SAV approach has proven to be effective to simulate the dynamics of gradient flows, would it be still effective for computing the steady state solutions of gradient flows?

The main purpose of this paper is to construct efficient schemes based on the SAV approach for the imaginary time gradient flow of one- and multi-component BECs, with or without normalization. In order to deal with the norm constraint, we adapt the SAV approach with an additional penalty term in the free energy to enforce the norm constraint, thus avoiding the complicated projection onto the constrained subspace in the multi-component cases. Two types of SAV schemes are proposed: the first is based on the original SAV scheme for the imaginary time gradient flow of BECs which is accurate for the dynamic evolution but may converge slowly towards stationary solutions; the second is a modified SAV scheme based on the normalized imaginary time gradient flow and leads to fast convergence towards stationary solutions. Both schemes require solving only linear elliptic problems with time independent coefficients or even constant coefficients at each time step, so they are very efficient and easy to implement.

The rest of the paper is organized as follows. In Section 2, we describe the SAV schemes for the imaginary time gradient flow of one-dimensional BECs. While these SAV schemes possess nice energy diminishing properties, they are not very efficient for computing the stationary solutions. Then, we consider in section 3 the modified SAV schemes for the normalized imaginary time gradient flow, which are very effective for computing the stationary solutions. In Section 4, we extend the results in Sections 2 and 3 to multi-component BECs. Some conclusions are given in Section 5.

## 2. The SAV approach for imaginary time gradient flow for one-component BECs

Let  $\Omega = \mathbb{R}^d$  ( $d = 1, 2, 3$ ), and  $(\cdot, \cdot)$  be the inner product in  $L^2(\mathbb{R}^d)$ . Given a nonlinear potential function  $F(\phi)$ , e.g.,  $F(\phi) = \frac{\beta}{2}\phi^2$ , and a positive definite operator  $\mathcal{L}$ :  $\mathcal{L}\phi = (-\frac{1}{2}\Delta + V(x))\phi$  with  $V(x) \geq 0$ . We consider the one-component BEC system with the free energy

$$E(\phi) = \frac{1}{2}(\phi, \mathcal{L}\phi) + \frac{1}{2} \int_{\Omega} F(|\phi|^2) dx, \tag{2.1}$$

subject to the constraint

$$\int_{\Omega} |\phi(x)|^2 dx = 1.$$

The ground states of one-component BECs are the minimizers of the above free energy. A common approach is to solve the minimization problem by finding the stationary solutions for the following imaginary time gradient flow:

$$\begin{cases} \phi_t = -\frac{\delta E(\phi)}{\delta \phi} = -\mathcal{L}\phi - F'(|\phi|^2)\phi, & x \in \Omega, \quad t > 0, \\ \lim_{|x| \rightarrow \infty} \phi(x, t) = 0, & t \geq 0, \\ \int_{\Omega} |\phi(x, t)|^2 dx = 1, & t \geq 0. \end{cases} \tag{2.2}$$

We shall adopt the SAV approach coupled with a penalty term which has proven to be effective to enforce volume and surface area constraints in the phase-field vesicle membrane model [12]. More precisely, we consider the penalized energy

$$\widehat{E}(\phi) = \frac{1}{2}(\phi, \mathcal{L}\phi) + \frac{1}{2} \int_{\Omega} F(|\phi|^2) dx + \frac{1}{4\varepsilon} \left( \int_{\Omega} |\phi|^2 dx - 1 \right)^2, \tag{2.3}$$

where  $\varepsilon \ll 1$ , and the corresponding gradient flow

$$\phi_t = -\frac{\delta \widehat{E}(\phi)}{\delta \phi} = -(\mathcal{L}\phi + F'(|\phi|^2)\phi) + \frac{1}{\varepsilon} (|\phi|^2 - 1)\phi. \tag{2.4}$$

We first reformulate it by introducing two scalar auxiliary variables:

$$u = \sqrt{\int_{\Omega} F(|\phi|^2) dx + C_0} \quad (C_0 \geq 0), \quad v = \int_{\Omega} |\phi|^2 dx - 1.$$

Then, we can rewrite (2.4) as

$$\begin{cases} \phi_t = -(\mathcal{L}\phi + u \frac{\delta u}{\delta \phi} + \frac{1}{2\varepsilon} v \frac{\delta v}{\delta \phi}), \\ u_t = \int_{\Omega} \frac{\delta u}{\delta \phi} \phi_t dx, \\ v_t = \int_{\Omega} \frac{\delta v}{\delta \phi} \phi_t dx, \end{cases} \quad (2.5)$$

where

$$\frac{\delta u}{\delta \phi} = \frac{1}{2\sqrt{\int_{\Omega} F(|\phi|^2) dx + C_0}} F'(|\phi|^2) 2\phi, \quad \frac{\delta v}{\delta \phi} = 2\phi. \quad (2.6)$$

Since we are interested in the steady state solution of (2.5), we consider the following first-order SAV scheme:

$$\begin{cases} \frac{\phi^{n+1} - \phi^n}{\tau} = -\mathcal{L}\phi^{n+1} - u^{n+1} \cdot \frac{\delta u}{\delta \phi}(\phi^n) - \frac{1}{2\varepsilon} v^{n+1} \frac{\delta v}{\delta \phi}(\phi^n), \\ \frac{u^{n+1} - u^n}{\tau} = \int_{\Omega} \frac{\delta u}{\delta \phi}(\phi^n) \frac{\phi^{n+1} - \phi^n}{\tau} dx, \\ \frac{v^{n+1} - v^n}{\tau} = \int_{\Omega} \frac{\delta v}{\delta \phi}(\phi^n) \frac{\phi^{n+1} - \phi^n}{\tau} dx. \end{cases} \quad (2.7)$$

Taking the inner product of the first equation of (2.7) with  $\phi^{n+1} - \phi^n$ , and multiplying the second and third equation with  $u^{n+1}$  and  $\frac{1}{2\varepsilon} v^{n+1}$ , respectively, we obtain immediately the following:

**Theorem 2.1.** *The scheme (2.7) is unconditionally energy diminishing in the sense that*

$$\begin{aligned} \tilde{E}(\phi^{n+1}, u^{n+1}, v^{n+1}) - \tilde{E}(\phi^n, u^n, v^n) &= -\frac{2}{\tau} \|\phi^{n+1} - \phi^n\|^2 \\ &\quad - \left[ (\mathcal{L}(\phi^{n+1} - \phi^n), \phi^{n+1} - \phi^n) + (u^{n+1} - u^n)^2 + \frac{1}{2\varepsilon} (v^{n+1} - v^n)^2 \right], \end{aligned}$$

where  $\tilde{E}(\phi, u, v)$  is the modified energy, which is defined as

$$\tilde{E}(\phi, u, v) = (\mathcal{L}\phi, \phi) + u^2 + \frac{1}{2\varepsilon} v^2.$$

Next we show that the scheme (2.7) can be efficiently solved. Indeed, we can write it as a matrix system

$$\begin{pmatrix} I + \tau \mathcal{L} & * & * \\ * & 1 & 0 \\ * & 0 & 1 \end{pmatrix} \begin{pmatrix} \phi^{n+1} \\ u^{n+1} \\ v^{n+1} \end{pmatrix} = \bar{b}^n,$$

where  $I$  is the identity operator,  $*$  represents the terms with non-constant coefficients,  $\bar{b}^n$  includes only the terms from previous time steps. We can first solve  $(u^{n+1}, v^{n+1})^t$  using a block Gaussian elimination, which requires solving two systems of the form

$$\begin{cases} (I + \tau \mathcal{L})\psi = g(x), & x \in \Omega, \quad t > 0, \\ \lim_{|x| \rightarrow \infty} \psi(x) = 0, & t \geq 0. \end{cases} \quad (2.8)$$

With  $(u^{n+1}, v^{n+1})^t$  known, we can obtain  $\phi^{n+1}$  by solving one more system in the above form.

Several remarks are in order:

- At each time step, we need to solve the equation (2.8) where the variable coefficient  $V(x)$  does not change from one step to another. Therefore, one can pre-factorize the system matrix once and use it for every time step. This is a main advantage of the current approach compared with existing approaches such as the backward Euler finite difference method (BEFD) in [8].

**Table 1**  
Iteration numbers and energies with different  $\tau$ .

$\tau$	$K(\text{TSSP})$	$E_\beta(\text{TSSP})$	$K(\text{BEFD})$	$E_\beta(\text{BEFD})$	$K(\text{SAV1})$	$E_\beta(\text{SAV1})$	$K(\text{SAV2})$	$E_\beta(\text{SAV2})$
$10^{-1}$	44	6.402150	40	6.075935	61	10.84403	29	21.03350
$10^{-2}$	258	6.081956	195	6.075947	263	6.403377	230	6.217449
$10^{-3}$	1532	6.076198	1474	6.076074	1519	6.108345	1465	6.077424
$10^{-4}$	11318	6.077412	11299	6.077382	11315	6.080623	11292	6.077404

- One may use a different energy splitting in the SAV approach, e.g., put the potential term together with the nonlinear term  $F'(|\phi|^2)\phi$ . The corresponding SAV scheme will still be unconditionally energy diminishing. However, it only requires solving (2.8) with  $\mathcal{L} = -\Delta$  which is a problem with constant coefficient so that it can be solved even more efficiently by fast Poisson solvers. But it may also require smaller time steps to obtain accurate approximations.
- In all our computations, to avoid artificial domain truncation, we use a Hermite-spectral method [18] to solve the problem (2.8) in the whole space.

A second-order SAV scheme based on BDF2 can also be constructed as follows:

$$\begin{cases} \frac{3\phi^{n+1} - 4\phi^n + \phi^{n-1}}{2\tau} = -\mathcal{L}\phi^{n+1} - u^{n+1} \frac{\delta u}{\delta \phi}(\tilde{\phi}^{n+1}) - \frac{1}{2\varepsilon} v^{n+1} \frac{\delta v}{\delta \phi}(\tilde{\phi}^{n+1}), \\ 3u^{n+1} - 4u^n + u^{n-1} = \int_{\Omega} \frac{\delta u}{\delta \phi}(\tilde{\phi}^{n+1}) \cdot (3\phi^{n+1} - 4\phi^n + \phi^{n-1}) dx, \\ (3v^{n+1} - 4v^n + v^{n-1}) = \int_{\Omega} \frac{\delta v}{\delta \phi}(\tilde{\phi}^{n+1}) (3\phi^{n+1} - 4\phi^n + \phi^{n-1}) dx, \end{cases} \quad (2.9)$$

where  $\tilde{\phi}^{n+1} = 2\phi^n - \phi^{n-1}$ . It is easy to show that the scheme (2.9) is also unconditionally energy diminishing (cf. [21]).

### 2.1. Numerical results

We first compare the iteration number  $K$  and energy  $E_\beta(\phi) = 2E(\phi)$  of the SAV discretization (2.7) (SAV1) and (2.9) (SAV2) with those by the time-splitting sine-spectral method (TSSP) and BEFD used in [8]. We set

$$V(x) = \frac{x^2}{2}, \beta = 60, \phi_0(x) = \frac{e^{-x^2/2}}{(\pi)^{1/4}}.$$

For the TSSP method and BEFD method, the domain is truncated as  $(-8, 8)$  and then divided into  $N = 512$  equal intervals. The corresponding mesh size and mesh points are

$$h_x = \frac{1}{32}, x_i = -8 + i \cdot h_x, i = 0, 1, \dots, N.$$

For the SAV schemes, we set  $\varepsilon = 10^{-8}$ , and use a Hermite spectral method with  $N = 256$  Hermite-gauss points.

The stopping criterion for the steady state solution is  $|E_\beta(\phi^n) - E_\beta(\phi^{n+1})| < 10^{-6}$ .

The computational results are listed in Table 1. We observe from the table that BEFD is the most efficient and accurate, SAV1 and SAV2 become comparable only with very small time steps. The performance of SAV1 and SAV2 are comparable with SAV2 being slightly better than SAV1.

We also plot in Fig. 1 the evolution of the original energy  $E_\beta(\phi)$  and the modified energy  $\tilde{E}(\phi, u, v)$  by SAV1 with different time step. We observe that both energies are diminishing, although one can only prove that the modified energy is diminishing, and they all reach steady at approximately  $t = 1$  with different time steps. The errors of norm conservation, i.e., values of  $|\|\phi\|^2 - 1|$ , at the steady states with  $\tau = 0.01, 0.001, 0.0001$  are  $0.0319, 0.0032, 3.1943 \times 10^{-4}$ , respectively. These results are consistent with the fact that the SAV scheme SAV1 is a first-order scheme for the time-dependent problem (2.2).

It is clear from the above results that the SAV schemes SAV1 and SAV2 are not competitive compared with BEFD for computing the ground state of BECs. This is because that the SAV schemes SAV1 and SAV2 are designed to simulate the dynamics of (2.2), without special acceleration to find stationary solutions.

### 3. The modified SAV approach for normalized imaginary time gradient flow for one-component BECs

The time-splitting sine-spectral method (TS) and backward Euler finite difference method (BE) in [8] are discretizations of the following normalized imaginary time gradient flow [1,8,13]: Given  $\tau$  and set  $t_k = k\tau$  for all  $k \geq 0$ , solve

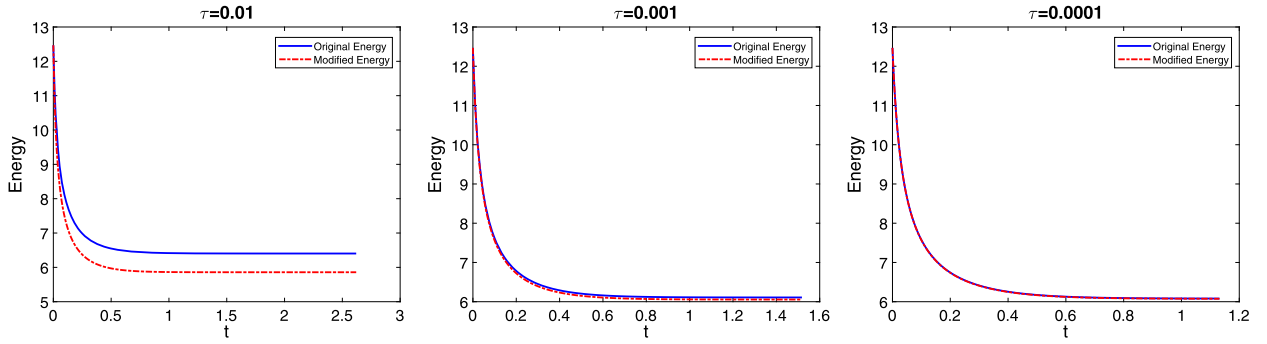


Fig. 1. Evolution of original and modified energies by the scheme SAV1.

$$\begin{cases} \phi_t = -\frac{\delta E(\phi)}{\delta \phi} = -\mathcal{L}\phi - F'(|\phi|^2)\phi, & x \in \Omega, t_n < t < t_{n+1}, \forall n \geq 0, \\ \lim_{|x| \rightarrow \infty} \phi(x, t) = 0, & t \geq 0, \\ \phi(x, t_{n+1}) := \phi(x, t_{n+1}^+) = \frac{\phi(x, t_{n+1}^-)}{\|\phi(\cdot, t_{n+1}^-)\|}, & x \in \Omega, \forall n \geq 0. \end{cases} \quad (3.1)$$

Bao and Du considered in [8] different time discretizations for (3.1), and concluded that the backward-Euler finite-difference (BEFD) and the time-splitting sine-spectral (TSSP) methods are the most effective. In particular, the backward-Euler finite-difference (BEFD) scheme is based on the following semi-implicit scheme for (3.1):

$$\begin{cases} \frac{\phi_*^{n+1} - \phi^n}{\tau} = -\mathcal{L}\phi_*^{n+1} - F'(|\phi^n|^2)\phi_*^{n+1}, \\ \phi^{n+1} = \frac{\phi_*^{n+1}}{\|\phi_*^{n+1}\|}. \end{cases} \quad (3.2)$$

The above scheme is linear but involves different variable coefficients at each time step.

### 3.1. Modified SAV schemes

In order to improve the performance of the SAV schemes SAV1, we propose the following modified SAV scheme (MSAV1) which is a first-order discretization of (3.1):

- Solve  $(\phi^{n+1}, \tilde{u}^{n+1}, \tilde{v}^{n+1})$  from

$$\begin{cases} \frac{\phi^{n+1} - \phi^n}{\tau} = -\mathcal{L}\phi^{n+1} - \tilde{u}^{n+1} \cdot \frac{\delta u}{\delta \phi}(\phi^n) - \frac{1}{2\varepsilon} \tilde{v}^{n+1} \frac{\delta v}{\delta \phi}(\phi^n), \\ \frac{\tilde{u}^{n+1} - u^n}{\tau} = \int_{\Omega} \frac{\delta u}{\delta \phi}(\phi^n) \frac{\phi^{n+1} - \phi^n}{\tau} dx, \\ \frac{\tilde{v}^{n+1} - v^n}{\tau} = \int_{\Omega} \frac{\delta v}{\delta \phi}(\phi^n) \frac{\phi^{n+1} - \phi^n}{\tau} dx. \end{cases} \quad (3.3)$$

- Update  $u^{n+1}$  and  $v^{n+1}$  via

$$u^{n+1} = \sqrt{\int_{\Omega} F(|\phi^{n+1}|^2) dx}, \quad v^{n+1} = \int_{\Omega} |\phi^{n+1}|^2 dx - 1. \quad (3.4)$$

Similarly, a modified second-order SAV scheme (MSAV2) is:

**Table 2**  
Iteration numbers and energies of the modified SAV schemes with different  $\tau$ .

$\tau$	$K(\text{MSAV1})$	$E_\beta(\text{MSAV1})$	$K(\text{MSAV2})$	$E_\beta(\text{MSAV2})$
$10^{-1}$	41	6.075943	840	6.651923
$10^{-2}$	195	6.075956	180	6.075955
$10^{-3}$	1474	6.076084	1463	6.076082
$10^{-4}$	11301	6.077390	11292	6.077390

- Solve  $(\phi^{n+1}, \tilde{u}^{n+1}, \tilde{v}^{n+1})$  from

$$\begin{cases} \frac{3\phi^{n+1} - 4\phi^n + \phi^{n-1}}{2\tau} = -\mathcal{L}\phi^{n+1} - \tilde{u}^{n+1} \frac{\delta u}{\delta \phi}(\tilde{\phi}^{n+1}) - \frac{1}{2\varepsilon} \tilde{v}^{n+1} \frac{\delta v}{\delta \phi}(\tilde{\phi}^{n+1}), \\ 3\tilde{u}^{n+1} - 4u^n + u^{n-1} = \int_{\Omega} \frac{\delta u}{\delta \phi}(\tilde{\phi}^{n+1}) \cdot (3\phi^{n+1} - 4\phi^n + \phi^{n-1}) dx, \\ (3\tilde{v}^{n+1} - 4v^n + v^{n-1}) = \int_{\Omega} \frac{\delta v}{\delta \phi}(\tilde{\phi}^{n+1}) (3\phi^{n+1} - 4\phi^n + \phi^{n-1}) dx, \end{cases} \quad (3.5)$$

- Update  $u^{n+1}$  and  $v^{n+1}$  via (3.4).

Note that the first step of the modified schemes MSAV1 and MSAV2 is simply the original SAV schemes SAV1 and SAV2, respectively. We derive immediately from Theorem 2.1 that

**Corollary 3.1.** For the scheme (3.3), we have

$$\begin{aligned} \tilde{E}(\phi^{n+1}, \tilde{u}^{n+1}, \tilde{v}^{n+1}) - \tilde{E}(\phi^n, u^n, v^n) &= -\frac{2}{\tau} \|\phi^{n+1} - \phi^n\|^2 \\ &\quad - \left[ (\mathcal{L}(\phi^{n+1} - \phi^n), \phi^{n+1} - \phi^n) + (\tilde{u}^{n+1} - u^n)^2 + \frac{1}{2\varepsilon} (\tilde{v}^{n+1} - v^n)^2 \right], \end{aligned}$$

where  $\tilde{E}(\phi, u, v)$  is the modified energy defined as

$$\tilde{E}(\phi, u, v) = (\mathcal{L}\phi, \phi) + u^2 + \frac{1}{2\varepsilon} v^2.$$

**Remark 3.1.** The above result does not imply that the scheme (3.3)-(3.4) is energy diminishing, since we can not prove  $\tilde{E}(\phi^{n+1}, u^{n+1}, v^{n+1}) - \tilde{E}(\phi^n, u^n, v^n) \leq 0$ .

Similar result holds for the second-order scheme (3.5)-(3.4).

Table 2 shows the computational results using these two modified schemes. The computational parameters are the same as in Table 1 for the schemes (2.7) and (2.9). We observe that the performance of MSAV1 is essentially the same as BEFD, and that MSAV2 also improved significantly over SAV2. However, our modified schemes only involve, at each time step, solving linear differential equation of the type (2.8). On the other hand, the BEFD scheme involves solving a linear problem with different variable coefficients at each time step. So our MSAV1 scheme is computationally more efficient than the BEFD scheme (3.2).

We also plot in Fig. 2 the evolution of the original energy  $E_\beta(\phi)$  and modified energy  $\tilde{E}(\phi, u, v)$  by the modified scheme MSAV1 with different time step. Note that the two energies diminish and stay together at all times, and reach steady state quickly. As for the  $L^2$ -norm conservation, the values of  $|\|\phi\|^2 - 1|$  at the steady states with  $\tau = 0.01, 0.001, 0.0001$  are  $9.4566 \times 10^{-8}, 1.0014 \times 10^{-7}, 1.0107 \times 10^{-7}$  which are much smaller than those given by SAV1. Therefore, we shall always use MSAV1 for the rest of the computation.

Table 3 list the required iteration number by the MSAV1 scheme with different time step  $\tau$  and penalty parameter  $\varepsilon$ . We observe that the required iteration number is not sensitive with  $\varepsilon$ . However, the required iteration number grows linearly as we decrease the time step. Therefore, the scheme is more efficient with larger time steps.

Next, we examine how the  $L^2$ -norm is preserved with different  $\varepsilon$  and  $\beta$ .

To fix the idea, we take  $\phi_0(x) = \frac{1}{\pi^{1/4}} e^{-x^2/2}, V(x) = \frac{x^2}{2}, \tau = 0.001$ . Then

- choose  $\beta = 10, 60, 100$ , and let  $\varepsilon$  vary from  $10^{-9}$  to  $10^{-1}$ . The results are shown in the left of Fig. 3.
- choose  $\varepsilon = 10^{-9}, 10^{-8}, 10^{-7}, 10^{-6}$ , and let  $\beta$  vary from  $10^0$  to  $10^4$ . The results are shown in the right of Fig. 3.

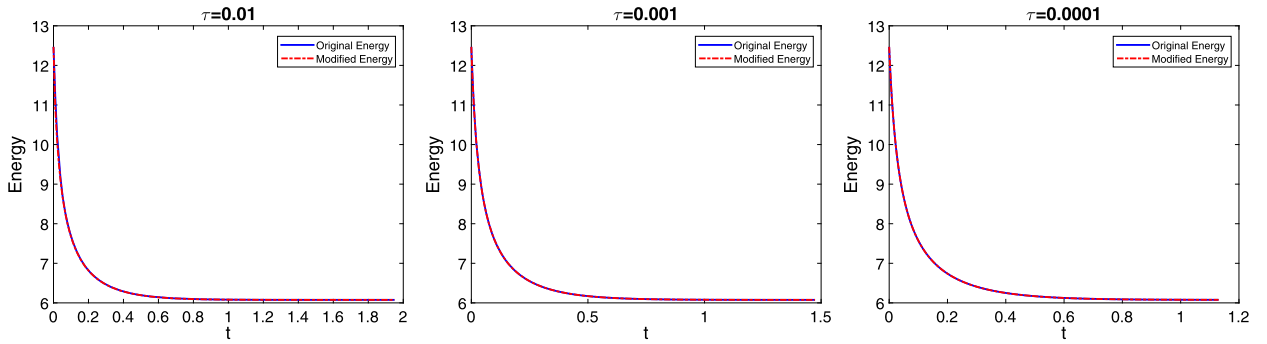


Fig. 2. Evolution of original and modified energies by the MSAV1 scheme.

Table 3  
Iteration numbers with different  $\tau$  and  $\epsilon$ .

$\tau \setminus \epsilon$	$10^{-10}$	$10^{-9}$	$10^{-8}$	$10^{-7}$	$10^{-6}$	$10^{-5}$	$10^{-4}$	$10^{-3}$
0.1	39	38	41	41	41	41	40	34
0.01	180	195	195	195	195	195	193	174
0.001	1440	1472	1474	1475	1475	1474	1468	1404
0.0001	11253	11296	11301	11300	11300	11298	11274	11035

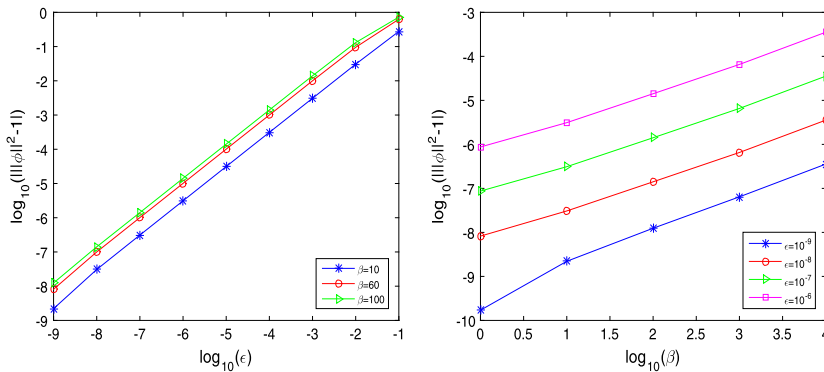


Fig. 3. Left:  $\|\phi(x)\|^2 - 1$  Vs.  $\epsilon$ ; Right:  $\|\phi(x)\|^2 - 1$  Vs.  $\beta$ .

Table 4  
Maximum errors  $\max|\phi_g - \phi_\epsilon|$  with different  $\epsilon$  and  $\beta$ . In this table, the stopping criterion for the steady state solution is  $\max|\phi_\epsilon^n - \phi_\epsilon^{n+1}| < 10^{-9}$ .

$\epsilon \setminus \beta$	1	10	100	500	1000	1500
$10^{-6}$	6.0903e-07	1.0957e-06	4.2453e-06	1.3014e-05	2.1087e-05	2.8347e-05
$10^{-5}$	2.5104e-06	8.5500e-06	4.1057e-05	1.2907e-04	2.1009e-04	2.8229e-04
$10^{-4}$	2.7257e-05	8.3442e-05	4.0891e-04	0.0013	0.0021	0.0028
$10^{-3}$	2.7569e-04	8.3184e-04	0.0041	0.0126	0.0204	0.0265
$10^{-2}$	0.0028	0.0082	0.0384	0.0967	0.1210	0.1314
$10^{-1}$	0.0274	0.0736	0.2083	0.2345	0.2251	0.2168

It is clear seen from the figures that the value of  $\|\phi\|^2 - 1$  depends linearly on  $\epsilon$  and  $\beta$ . In particular,  $\epsilon$  should be proportionally decreased as  $\beta$  increases to preserve the accuracy on  $L^2$ -norm conservation.

Next, we make a detailed comparison between the numerical ground state  $\phi_\epsilon$  via the SAV scheme (MSAV1) and the exact ground state  $\phi_g$  as  $\epsilon \rightarrow 0$ . The results are listed in Table 4. We observe that the accuracy improves linearly as  $\epsilon$  decreases, i.e.,  $\max|\phi_g - \phi_\epsilon| \approx O(\epsilon)$  for any given  $\beta$ .

### 3.2. Ground state solution and first excited state solution in one-dimension

In order to further validate the scheme MSAV1, we use it to compute the ground state solution and first excited state solution of a well studied case.

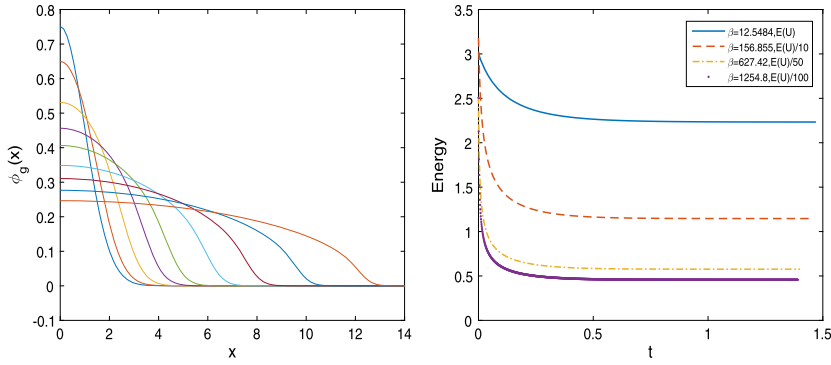


**Fig. 4.** Left: Ground state solution for  $\beta = 0, 3.1371, 12.5484, 31.371, 62.742, 156.855, 313.71, 627.42, 1254.8$  (with decreasing peak). Right: Energy evolution  $E_\beta(\phi)$  for different  $\beta$ .

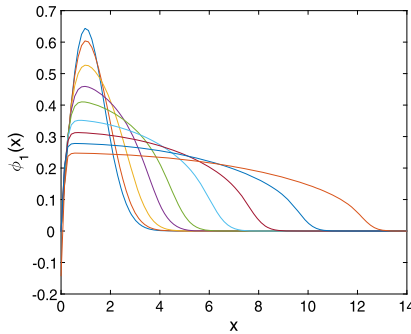


**Fig. 5.** First excited state solution  $\phi_1(x)$  for  $\beta = 0, 3.1371, 12.5484, 31.371, 62.742, 156.855, 313.71, 627.42, 1254.8$  (with decreasing peak).

**Example 3.1.** Ground state solutions of BECs with harmonic oscillator potential

$$V(x) = \frac{x^2}{2}, \quad \phi_0(x) = \frac{1}{\pi^{1/4}} e^{-x^2/2}, \quad x \in R.$$

The numerical parameters in the computation are

$$N = 256, \quad \varepsilon = 10^{-8}, \quad \tau = 0.001.$$

We show in Fig. 4 the ground state solution  $\phi_g(x)$  and energy evolution for different  $\beta$ . The results are in good qualitative agreement with those obtained by directly minimizing the energy functional [10] and the TS method in [8].

The scheme can also be used to compute the first excited state solution of BECs.

**Example 3.2.** First excited state solutions of BECs with harmonic oscillator potential

$$V(x) = \frac{x^2}{2}, \quad \phi_0(x) = \frac{\sqrt{2}}{\pi^{1/4}} x e^{-x^2/2}, \quad x \in R.$$

We still take the discretization parameters to be  $N = 256, \varepsilon = 10^{-8}, \tau = 0.001$ . Fig. 5 shows the first excited state solution  $\phi_1(x)$  with different  $\beta$ . The results are in good agreement with those computed in [10] and [8].

In order to make a quantitative comparison, we compute the chemical potential and the energy of the ground state solution and the first excited state solution. Given  $\phi$ , the chemical potential  $\mu$  can be computed by

$$\begin{aligned} \mu &= \mu_\beta(\phi) = \int_{\Omega} \left[ \frac{1}{2} |\nabla \phi(x)|^2 + V(x) |\phi(x)|^2 + \beta |\phi(x)|^4 \right] dx \\ &= E_\beta(\phi) + \int_{\Omega} \frac{\beta}{2} |\phi(x)|^4 dx. \end{aligned}$$

Let  $\phi_g$  and  $\phi_1$  be the ground state solution and the first excited state solution, respectively. We set  $x_{rms} = \|x\phi_1\|_{L^2(\Omega)}$  be the radius mean square of  $\phi_1(x)$ ,  $E_\beta(\phi_g)$  and  $E_\beta(\phi_1)$  be the corresponding energy, and  $\mu_g = \mu_\beta(\phi_g)$  and  $\mu_1 = \mu_\beta(\phi_1)$ . Table 5



**Table 5**  
Chemical potentials and energies of the first excited state solution and the ground state solution.

$\beta$	$x_{rms}$	$E_\beta(\phi_g)$	$E_\beta(\phi_1)$	$\frac{E_\beta(\phi_1)}{E_\beta(\phi_g)}$	$\mu_g$	$\mu_1$	$\frac{\mu_1}{\mu_g}$
0	1.2247	0.5000	1.5000	3.0000	0.5000	1.5000	3.0000
3.1371	1.3132	1.0441	1.9414	1.8594	1.5285	2.3589	1.5433
12.5484	1.5413	2.2330	3.0377	1.3604	3.5997	4.3470	1.2076
31.371	1.8619	3.9810	4.7437	1.1916	6.5563	7.2836	1.1109
62.742	2.2239	6.2570	6.9997	1.1187	10.3735	11.0930	1.0694
156.855	2.8958	11.4645	12.1912	1.0634	19.0750	19.7887	1.0374
313.71	3.5835	18.1710	18.8909	1.0396	30.2642	30.9773	1.0236
627.42	4.4657	28.8253	29.5433	1.0249	48.0297	48.7501	1.0150
1254.8	5.5811	45.7431	46.4368	1.0152	76.2325	76.8884	1.0086

shows the computational results. It is observed that this table agrees quantitatively with the Table 4.3 in [8]. In particular, we have

$$\lim_{\beta \rightarrow \infty} \frac{E_\beta(\phi_1)}{E_\beta(\phi_g)} = 1, \quad \lim_{\beta \rightarrow \infty} \frac{\mu_1}{\mu_g} = 1.$$

### 3.3. Ground state solution of BECs in two-dimension

Since the SAV schemes only involving solving equations of the type (2.8), so implementation in multi-dimensions is straightforward. We now apply the MSAV1 scheme to compute the ground state solutions of BECs in two-dimension. We take the initial condition to be

$$\phi_0(x, y) = \frac{(\gamma_x \gamma_y)^{1/4}}{\pi^{1/2}} e^{-(\gamma_x^2 x^2 + \gamma_y^2 y^2)/2},$$

with two different potential functions:

- Case 1. A harmonic oscillator potential [8–10,14]

$$V(x, y) = \frac{1}{2}(\gamma_x^2 x^2 + \gamma_y^2 y^2).$$

- Case 2. A harmonic oscillator potential and a potential of a stirrer corresponding to a far-blue detuned Gaussian laser beam [8,15]

$$V(x, y) = \frac{1}{2}(\gamma_x^2 x^2 + \gamma_y^2 y^2) + \omega_0 e^{-\delta((x-r_0)^2 + y^2)},$$

and the parameters are  $\gamma_x = 1, \gamma_y = 4$ , and  $\beta = 200$  in Case 1 and  $\gamma_x = 1, \gamma_y = 1, \omega_0 = 4, \delta = r_0 = 1$ , and  $\beta = 200$  in Case 2. We then solve the problem with the numerical parameters  $N = 128, \varepsilon = 10^{-8}, \tau = 0.01$ . We plot the ground state solutions of both cases in Fig. 6. Moreover, the chemical potential and energy corresponding to these ground states are

- Case 1:  $x_{rms} = 2.2812, y_{rms} = 0.6096, E_\beta(\phi_g) = 11.1560, \mu_g = 16.3002$ .
- Case 2:  $x_{rms} = 1.6978, y_{rms} = 1.7169, E_\beta(\phi_g) = 5.8506, \mu_g = 8.3189$ .

These results are also in excellent agreement with those reported in [8].

## 4. Multi-component BECs

To fix the idea, we shall only consider two-component BECs. The method presented below can be straightforwardly extended to deal with multi-component BECs [5].

We consider the two-component (pseudo spin-1/2) BEC system with Josephson junction [4,22] whose free energy is given by

$$\mathcal{E}(\phi_1, \phi_2) = \int \left( \frac{1}{2} |\nabla \phi_1|^2 + \frac{1}{2} |\nabla \phi_2|^2 \right) + V_1(x) |\phi_1|^2 + V_2(x) |\phi_2|^2 dx + \mathcal{E}_0(\phi_1, \phi_2), \tag{4.1}$$

where

$$\mathcal{E}_0(\phi_1, \phi_2) = \int \left[ \frac{1}{2} \beta_{11} |\phi_1|^4 + \frac{1}{2} \beta_{22} |\phi_2|^4 + \beta_{12} |\phi_1|^2 |\phi_2|^2 + \lambda \phi_1 \phi_2 + \frac{\delta}{2} (|\phi_1|^2 - |\phi_2|^2) \right] dx, \tag{4.2}$$

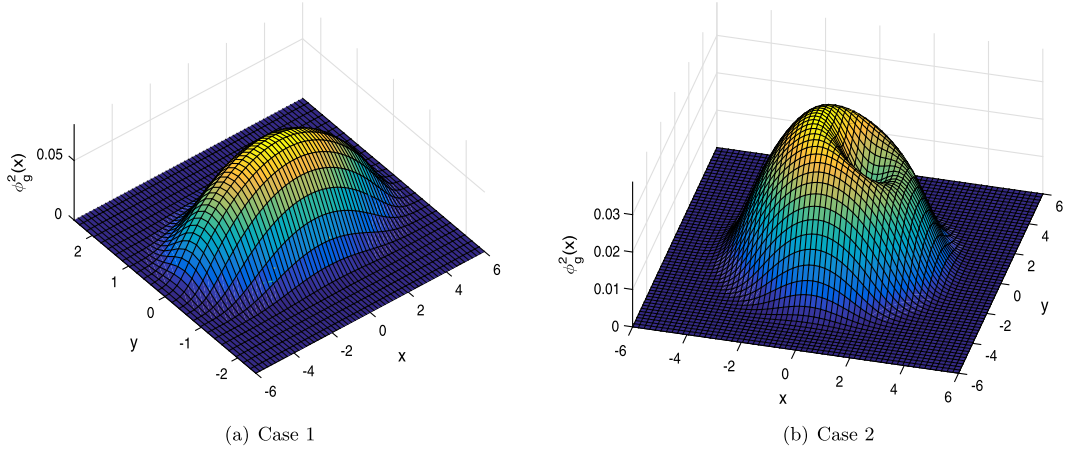


Fig. 6. Ground state solutions in the 2-D case.

subject to the constraint

$$\int_{\Omega} |\phi_1(x, t)|^2 dx + \int_{\Omega} |\phi_2(x, t)|^2 dx = 1, \quad t \geq 0. \tag{4.3}$$

In the above, the unknown functions  $(\phi_1, \phi_2)$  are the macroscopic wave function corresponding to the spin-up and spin-down components,  $V_i(x)$  ( $i = 1, 2$ ) are two external trapping potentials,  $\lambda$  is the effective Rabi frequency,  $\delta$  is the Raman transition constant,  $\beta_{ij}$  ( $i, j = 1, 2$ ) are related to the s-wave scattering lengths between  $i$ -th and  $j$ -th components (positive for repulsive interaction and negative for attractive interaction).

#### 4.1. SAV schemes for the imaginary time gradient flow

To minimize the above free energy, one can also use the corresponding imaginary time gradient flow:

$$\begin{cases} \frac{\partial \phi_1}{\partial t} = \left( \frac{1}{2} \Delta - V_1(x) - \frac{\delta}{2} - (\beta_{11} |\phi_1|^2 + \beta_{12} |\phi_2|^2) \right) \phi_1 - \frac{\lambda}{2} \phi_2, & x \in \Omega, \quad t > 0, \\ \frac{\partial \phi_2}{\partial t} = \left( \frac{1}{2} \Delta - V_2(x) + \frac{\delta}{2} - (\beta_{12} |\phi_1|^2 + \beta_{22} |\phi_2|^2) \right) \phi_2 - \frac{\lambda}{2} \phi_1, & x \in \Omega, \quad t > 0, \end{cases} \tag{4.4}$$

with the constraint (4.3).

As in the one-component case, we introduce two SAVs

$$u = \sqrt{\mathcal{E}_0(\phi_1, \phi_2) + C_0}, \quad v = \int_{\Omega} |\phi_1(x, t)|^2 dx + \int_{\Omega} |\phi_2(x, t)|^2 dx - 1,$$

where  $C_0$  is a constant such that  $\mathcal{E}_0(\phi_1, \phi_2) + C_0 > 0$ . Then, we can rewrite the problem (4.4)-(4.3) as:

$$\begin{cases} \frac{\partial \phi_1}{\partial t} = \left( \frac{1}{2} \Delta - V_1(x) \right) \phi_1 - u \frac{\delta u}{\delta \phi_1} - \frac{1}{2\epsilon} v \frac{\delta v}{\delta \phi_1}, \\ \frac{\partial \phi_2}{\partial t} = \left( \frac{1}{2} \Delta - V_2(x) \right) \phi_2 - u \frac{\delta u}{\delta \phi_2} - \frac{1}{2\epsilon} v \frac{\delta v}{\delta \phi_2}, \\ \frac{\partial u}{\partial t} = \int_{\Omega} \left( \frac{\delta u}{\delta \phi_1} \frac{\partial \phi_1}{\partial t} + \frac{\delta u}{\delta \phi_2} \frac{\partial \phi_2}{\partial t} \right) dx, \\ \frac{\partial v}{\partial t} = \int_{\Omega} \left( \frac{\delta v}{\delta \phi_1} \frac{\partial \phi_1}{\partial t} + \frac{\delta v}{\delta \phi_2} \frac{\partial \phi_2}{\partial t} \right) dx, \end{cases} \tag{4.5}$$

where

$$\begin{aligned}\frac{\delta u}{\delta \phi_1} &= \frac{1}{2\sqrt{\mathcal{E}_0(\phi_1, \phi_2)}} [(\beta_{11}|\phi_1|^2 + \beta_{12}|\phi_2|^2)2\phi_1 + \lambda\phi_2 + \delta\phi_1], \\ \frac{\delta u}{\delta \phi_2} &= \frac{1}{2\sqrt{\mathcal{E}_0(\phi_1, \phi_2)}} [(\beta_{12}|\phi_1|^2 + \beta_{22}|\phi_2|^2)2\phi_2 + \lambda\phi_1 - \delta\phi_2], \\ \frac{\delta v}{\delta \phi_1} &= 2\phi_1, \quad \frac{\delta v}{\delta \phi_2} = 2\phi_2.\end{aligned}$$

Then, a first-order SAV scheme for (4.5) is

$$\frac{\phi_1^{n+1} - \phi_1^n}{\tau} = \left(\frac{1}{2}\Delta - V_1(x)\right)\phi_1^{n+1} - r_{11}^n u^{n+1} - \frac{1}{2\varepsilon} r_{12}^n v^{n+1}, \quad (4.6a)$$

$$\frac{\phi_2^{n+1} - \phi_2^n}{\tau} = \left(\frac{1}{2}\Delta - V_2(x)\right)\phi_2^{n+1} - r_{21}^n u^{n+1} - \frac{1}{2\varepsilon} r_{22}^n v^{n+1}, \quad (4.6b)$$

$$u^{n+1} - u^n = \int_{\Omega} (r_{11}^n \cdot (\phi_1^{n+1} - \phi_1^n) + r_{21}^n \cdot (\phi_2^{n+1} - \phi_2^n)) dx, \quad (4.6c)$$

$$v^{n+1} - v^n = \int_{\Omega} (r_{12}^n \cdot (\phi_1^{n+1} - \phi_1^n) + r_{22}^n \cdot (\phi_2^{n+1} - \phi_2^n)) dx, \quad (4.6d)$$

where

$$\begin{aligned}r_{11}^n &= \frac{\delta u}{\delta \phi_1}(\phi_1^n, \phi_2^n), \quad r_{12}^n = \frac{\delta v}{\delta \phi_1}(\phi_1^n, \phi_2^n), \\ r_{21}^n &= \frac{\delta u}{\delta \phi_2}(\phi_1^n, \phi_2^n), \quad r_{22}^n = \frac{\delta v}{\delta \phi_2}(\phi_1^n, \phi_2^n).\end{aligned}$$

**Theorem 4.1.** The SAV scheme (4.6) is unconditionally energy diminishing in the sense that

$$\begin{aligned}\tilde{\mathcal{E}}(\phi_1^{n+1}, \phi_2^{n+1}, u^{n+1}, v^{n+1}) - \tilde{\mathcal{E}}(\phi_1^n, \phi_2^n, u^n, v^n) &= -\frac{2}{\tau} \|\phi_1^{n+1} - \phi_1^n\|^2 - \frac{2}{\tau} \|\phi_2^{n+1} - \phi_2^n\|^2 \\ &\quad - \tilde{\mathcal{E}}(\phi_1^{n+1} - \phi_1^n, \phi_2^{n+1} - \phi_2^n, u^{n+1} - u^n, v^{n+1} - v^n),\end{aligned}$$

where  $\tilde{\mathcal{E}}(\phi_1, \phi_2, u, v)$  is the modified energy

$$\tilde{\mathcal{E}}(\phi_1, \phi_2, u, v) = \int_{\Omega} \sum_{j=1}^2 \left( \frac{1}{2} |\nabla \phi_j|^2 + V_j |\phi_j|^2 \right) dx + u^2 + \frac{1}{2\varepsilon} v^2.$$

**Proof.** Taking the inner products of (4.6a) and (4.6b) with  $\phi_1^{n+1} - \phi_1^n$  and  $\phi_2^{n+1} - \phi_2^n$  respectively, and multiplying (4.6c) and (4.6d) with  $u^{n+1}$  and  $\frac{1}{2\varepsilon} v^{n+1}$ , respectively, we obtain

$$\begin{aligned}\frac{1}{\tau} \|\phi_1^{n+1} - \phi_1^n\|^2 + \frac{1}{\tau} \|\phi_2^{n+1} - \phi_2^n\|^2 &= -u^{n+1}(u^{n+1} - u^n) - \frac{1}{2\varepsilon} v^{n+1}(v^{n+1} - v^n) \\ &\quad + \left( \left( \frac{1}{2}\Delta - V_1(x) \right) \phi_1^{n+1}, \phi_1^{n+1} - \phi_1^n \right) + \left( \left( \frac{1}{2}\Delta - V_2(x) \right) \phi_2^{n+1}, \phi_2^{n+1} - \phi_2^n \right).\end{aligned}$$

Using the identity  $2(b - a, b) = |b|^2 - |a|^2 + |b - a|^2$ , the above equation can be rewritten as

$$\begin{aligned}\frac{1}{2} \tilde{\mathcal{E}}(\phi_1^{n+1}, \phi_2^{n+1}, u^{n+1}, v^{n+1}) - \frac{1}{2} \tilde{\mathcal{E}}(\phi_1^n, \phi_2^n, u^n, v^n) &= -\frac{1}{\tau} \|\phi_1^{n+1} - \phi_1^n\|^2 - \frac{1}{\tau} \|\phi_2^{n+1} - \phi_2^n\|^2 \\ &\quad - \frac{1}{2} \tilde{\mathcal{E}}(\phi_1^{n+1} - \phi_1^n, \phi_2^{n+1} - \phi_2^n, u^{n+1} - u^n, v^{n+1} - v^n),\end{aligned}$$

which implies the desired result.  $\square$

One can also easily construct second-order unconditionally energy diminishing SAV schemes based on Crank-Nicolson or BDF2.

As in the one-component case, the scheme (4.6) can also be efficiently implemented. To this end, we write scheme (4.6) as a matrix system

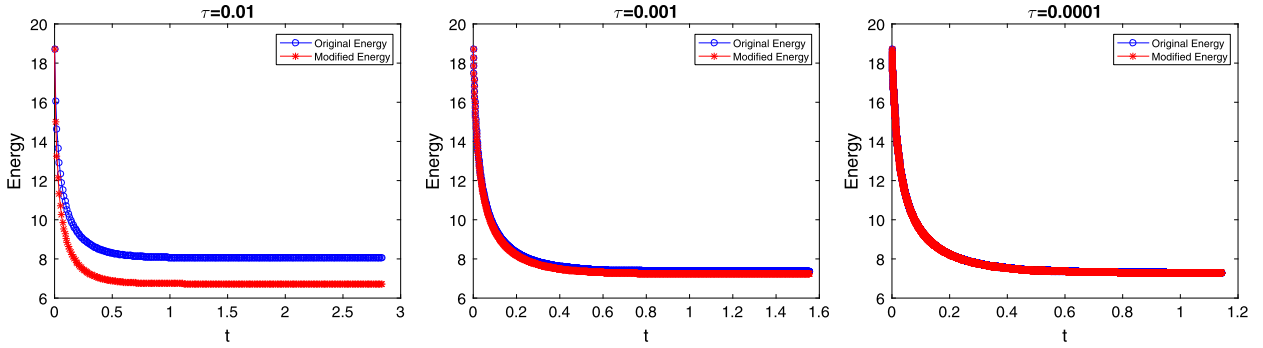


Fig. 7. Evolution of original and modified energies by SAV1 with  $\beta = 100$  and  $\lambda = -2$ .

$$\begin{pmatrix} I + \tau \mathcal{L}_1 & 0 & * & * \\ 0 & I + \tau \mathcal{L}_2 & * & * \\ * & * & 1 & 0 \\ * & * & 0 & 1 \end{pmatrix} \begin{pmatrix} \phi_1^{n+1} \\ \phi_2^{n+1} \\ u^{n+1} \\ v^{n+1} \end{pmatrix} = \bar{b}^n,$$

where  $I$  is the identity operator,  $\mathcal{L}_i \psi := (\frac{1}{2} \Delta - V_i(x)) \psi$  ( $i = 1, 2$ ),  $*$  represents the terms with non-constant coefficients,  $\bar{b}^n$  includes only the terms from previous time steps. We can first solve  $(u^{n+1}, v^{n+1})^t$  using a block Gaussian elimination, which requires solving two decoupled systems of the form ( $i = 1, 2$ ):

$$\begin{cases} (I + \tau \mathcal{L}_i) \psi_i(x) = g_i(x), & x \in \Omega, \quad t > 0, \\ \lim_{|x| \rightarrow \infty} \psi_i(x) = 0, & t \geq 0. \end{cases} \tag{4.7}$$

With  $(u^{n+1}, v^{n+1})^t$  known, we can obtain  $\phi^{n+1}$  by solving one more system in the above form. Hence, the solution procedures of the SAV schemes for the one- and two-component BECs are essentially the same. No extra efforts are needed for the two-component BECs.

4.2. Numerical results with the SAV scheme (4.6)

First, we use the SAV scheme (4.6) to compute the ground state of the following example.

**Example 4.1.** Let  $V_1(x) = V_2(x) = \frac{x^2}{2}$ ,  $\delta = 0$ , and  $\beta_{11} : \beta_{12} : \beta_{22} = (1 : 0.94 : 0.97)\beta$  with  $\beta$  to be specified. The initial conditions are taken to be

$$\phi_1^0(x) = \phi_2^0(x) = \frac{1}{\pi^{1/4} \sqrt{2}} e^{-x^2/2}.$$

The numerical parameters are  $\varepsilon = 10^{-8}$ ,  $\tau = 0.01$  and  $N = 512$ . We show in Fig. 7 evolutions of the original energy  $\mathcal{E}$  and modified energy  $\tilde{\mathcal{E}}$  with different time step by the scheme (4.6). We observe that both energies are diminishing, but they are only close for  $\tau$  very small. On the other hand, the values of  $|\|\phi_1\|^2 + \|\phi_2\|^2 - 1|$  at  $\tau = 0.01, 0.001, 0.0001$  are  $0.0569, 0.0057, 5.7008 \times 10^{-4}$  so the convergence of  $L^2$ -norm is also very slow. These results indicate that, similar to the one-component case, the scheme (4.8) is not very efficient for computing the ground state solutions for the two-component BECs. See also Table 6 for the required iteration numbers to reach the steady state and the energy at the steady state.

4.3. SAV schemes for the normalized imaginary time gradient flow

While it is easy to project the approximate solution to satisfy the norm constraint in the one-component case, it becomes much harder to do so for the two-component BECs [7]. However, the penalized SAV approach can still be easily applied to deal with the constraints for multi-component BECs.

As for the one-component case, we propose to use the following modified SAV scheme for (4.5):

- Solve  $\phi_1^{n+1}$  and  $\phi_2^{n+1}$  from the following equations

$$\frac{\phi_1^{n+1} - \phi_1^n}{\tau} = \left[ \frac{1}{2} \Delta - V_1(x) - \frac{\delta}{2} \right] \phi_1^{n+1} - r_{11}^n \tilde{u}^{n+1} + \frac{1}{2\varepsilon} r_{12}^n \tilde{v}^{n+1}, \tag{4.8a}$$

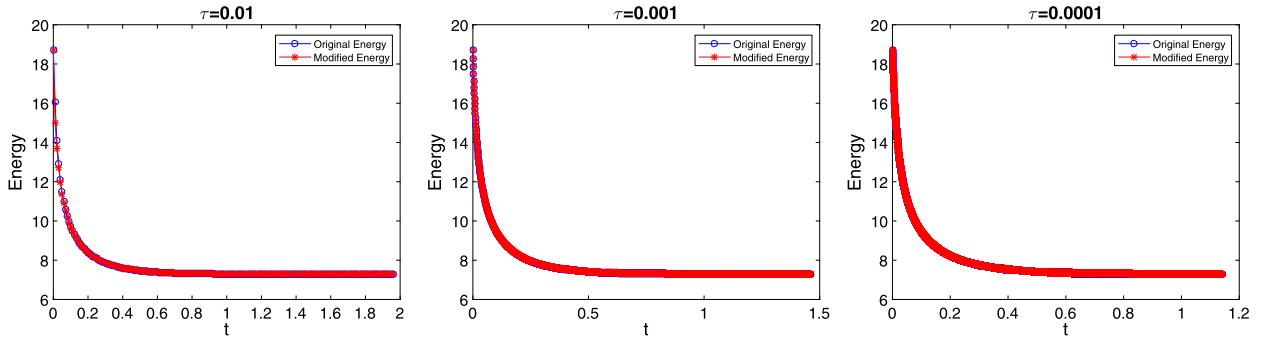


Fig. 8. Evolution of original and modified energies by modified SAV1 with  $\beta = 100$  and  $\lambda = -2$ .

$$\frac{\phi_2^{n+1} - \phi_2^n}{\tau} = \left[ \frac{1}{2} \Delta - V_2(x) + \frac{\delta}{2} \right] \phi_2^{n+1} - r_{21}^n \tilde{u}^{n+1} + \frac{1}{2\varepsilon} r_{22}^n \tilde{v}^{n+1}, \tag{4.8b}$$

$$\tilde{u}^{n+1} - u^n = \int_{\Omega} (r_{11}^n (\phi_1^{n+1} - \phi_1^n) + r_{21}^n (\phi_2^{n+1} - \phi_2^n)) dx, \tag{4.8c}$$

$$\tilde{v}^{n+1} - v^n = \int_{\Omega} (r_{12}^n (\phi_1^{n+1} - \phi_1^n) + r_{22}^n (\phi_2^{n+1} - \phi_2^n)) dx. \tag{4.8d}$$

- Update  $u^{n+1}$  and  $v^{n+1}$  via

$$u^{n+1} = \sqrt{\mathcal{E}_0(\phi_1^{n+1}, \phi_2^{n+1})}, \tag{4.9a}$$

$$v^{n+1} = \int_{\Omega} |\phi_1^{n+1}(x, t)|^2 dx + \int_{\Omega} |\phi_2^{n+1}(x, t)|^2 dx - 1. \tag{4.9b}$$

Note that the first step (4.8) is exactly the scheme (4.6). So the modified SAV scheme merely adds an update for  $u^{n+1}$  and  $v^{n+1}$  using the original energy and  $L^2$ -norm constraint at each time step. We derive immediately from Theorem 4.1 the following:

**Corollary 4.1.** For the scheme (4.8), we have

$$\begin{aligned} \tilde{\mathcal{E}}(\phi_1^{n+1}, \phi_2^{n+1}, \tilde{u}^{n+1}, \tilde{v}^{n+1}) - \tilde{\mathcal{E}}(\phi_1^n, \phi_2^n, u^n, v^n) &= -\frac{2}{\tau} \|\phi_1^{n+1} - \phi_1^n\|^2 - \frac{2}{\tau} \|\phi_2^{n+1} - \phi_2^n\|^2 \\ &\quad - \tilde{\mathcal{E}}(\phi_1^{n+1} - \phi_1^n, \phi_2^{n+1} - \phi_2^n, \tilde{u}^{n+1} - u^n, \tilde{v}^{n+1} - v^n), \end{aligned}$$

where  $\tilde{\mathcal{E}}(\phi_1, \phi_2, u, v)$  is the modified energy

$$\tilde{\mathcal{E}}(\phi_1, \phi_2, u, v) = \int_{\Omega} \sum_{j=1}^2 \left( \frac{1}{2} |\nabla \phi_j|^2 + V_j |\phi_j|^2 \right) dx + u^2 + \frac{1}{2\varepsilon} v^2.$$

#### 4.4. Numerical results using the modified SAV scheme (4.8)-(4.9)

We plot in Fig. 8 evolutions of the original energy  $\mathcal{E}$  and modified energy  $\tilde{\mathcal{E}}$  with different time step by the modified SAV scheme (4.8)-(4.9), and observe that the two energies stay close for all time steps and they converge to steady state quickly. The corresponding errors of  $L^2$ -norm conservation  $|\|\phi_1\|^2 + \|\phi_2\|^2 - 1|$  at  $\tau = 0.01, 0.001, 0.0001$  are respectively  $1.2410 \times 10^{-7}, 1.2726 \times 10^{-7}, 1.2813 \times 10^{-7}$ , which are independent of  $\tau$ . These results indicate that the modified SAV scheme (4.8) is very effective for computing the ground states of two-component BECs and conserves the  $L^2$ -norm well.

We list in Table 6 the required iteration numbers to reach the steady state and the energy at the steady state for both schemes SAV1 and MSAV1, and observe that the scheme MSAV1 is also very efficient and accurate in computing the ground state solutions of two-component BECs.

Next, we examine how the ground state depends on  $\lambda$  and  $\beta$ . Fig. 9 shows the ground state solutions with  $\beta = 100$  and different  $\lambda \leq 0$ . We observe that as  $\lambda$  decreases,  $\phi_1$  and  $\phi_2$  are getting closer and eventually converge towards each other as  $\lambda \rightarrow -\infty$ . Fig. 10 shows the ground state solutions with  $\lambda = -2$  and different  $\beta$ . We observe that as  $\beta$  increases,  $\phi_1$  and  $\phi_2$  are farther apart from each other.

Next, we consider the following example with highly oscillatory potentials:

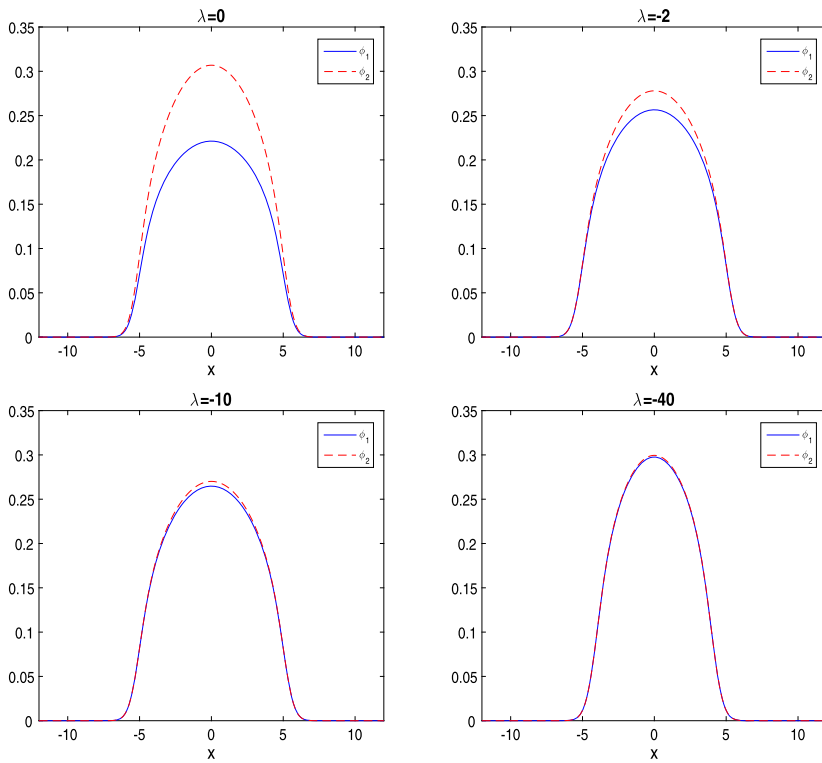


Fig. 9. Ground state solution with  $\beta = 100$  and different  $\lambda$ .

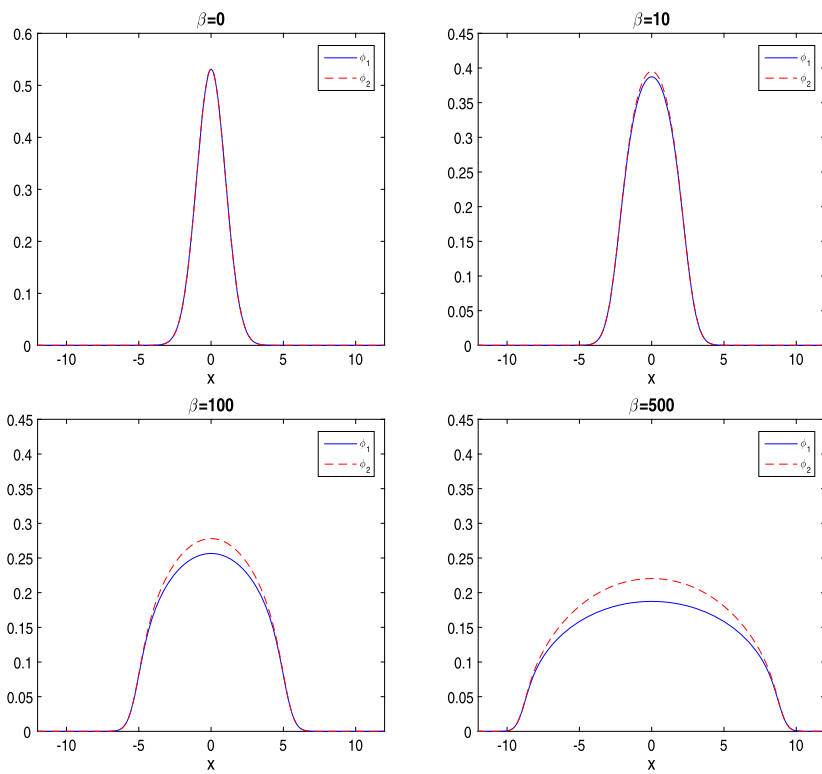
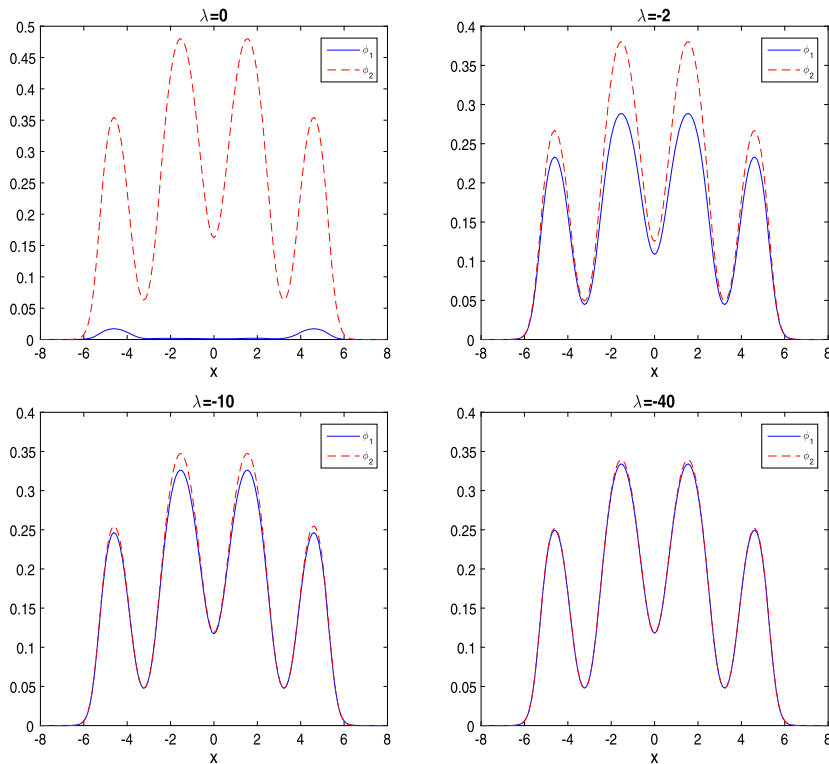


Fig. 10. Ground state solution with  $\lambda = -2$  and different  $\beta$ .

**Table 6**

Iteration number and energy of SAV1 and MSAV1 with different  $\tau$  for the case  $\beta = 100$  and  $\lambda = -2$  of the two-component BECs.

$\tau$	$K(\text{MSAV1})$	$\mathcal{E}(\text{MSAV1})$	$K(\text{SAV1})$	$\mathcal{E}(\text{SAV1})$
$10^{-2}$	196	7.293210	284	8.055077
$10^{-3}$	1461	7.293328	1555	7.366530
$10^{-4}$	11396	7.294530	11429	7.301847

**Fig. 11.** Ground state solution with  $\beta = 100$  and different  $\lambda$ .

**Example 4.2.** Let  $V_1(x) = V_2(x) = \frac{x^2}{2} + 24 \cos^2(x)$ ,  $\delta = 0$ , and  $\beta_{11} : \beta_{12} : \beta_{22} = (1.03 : 1 : 0.97)\beta$ . The initial conditions are taken to be

$$\phi_1^0(x) = \phi_2^0(x) = \frac{1}{\pi^{1/4}\sqrt{2}} e^{-x^2/2}.$$

We still use the same numerical parameters  $\varepsilon = 10^{-8}$ ,  $\tau = 0.01$  and  $N = 512$ .

We plot in Fig. 11 the ground state solutions with  $\beta = 100$  and different  $\lambda \leq 0$ , and in Fig. 12 the ground state solutions with  $\lambda = -2$  and different  $\beta$ . We observe similar behaviors as in the previous example as we decrease  $\lambda$  and increase  $\beta$ . These results are in full agreement with those in [6,7].

## 5. Concluding remarks

We constructed efficient and accurate schemes, based on the SAV approach coupled with a penalty term to enforce the norm constraint, for the imaginary time gradient flows of one- and multi-component BECs, with or without normalization, and applied them to compute stationary solutions of one- and two-component BECs. The SAV schemes without normalization are accurate for the dynamic evolution but may converge slowly towards stationary solutions, while the SAV schemes with normalization lead to fast convergence towards stationary solutions. Both schemes require solving only linear elliptic problems with time independent coefficients (or even constant coefficients if the potential term is treated explicitly) at each time step, and do not require projection onto the constrained subspace, so they are very efficient and easy to implement. These schemes also preserve the energy diminishing properties of the corresponding imaginary time gradient flows with or without normalization.

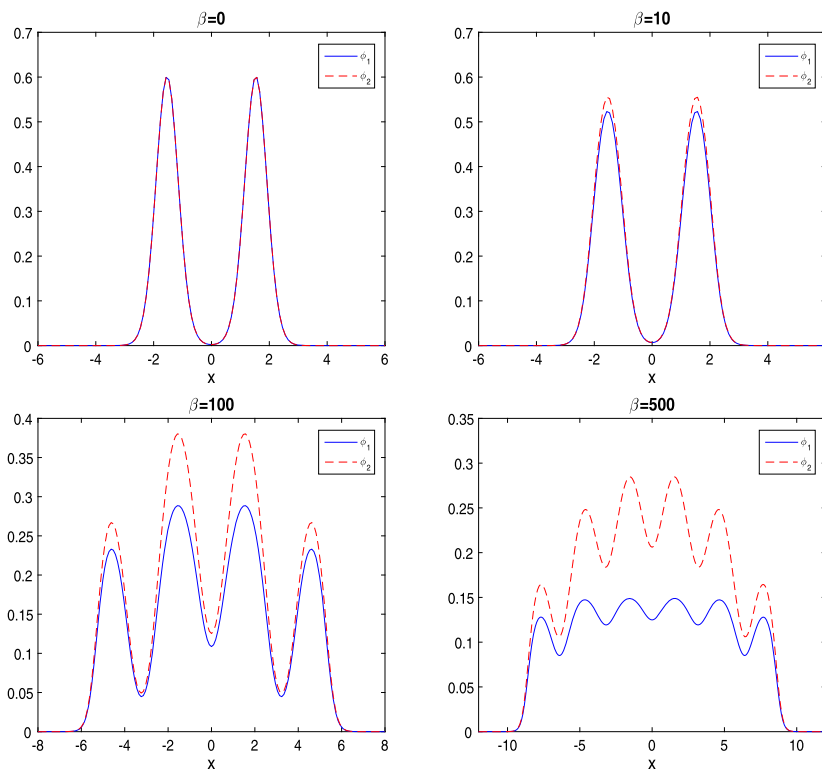


Fig. 12. Ground state solution with  $\lambda = -2$  and different  $\beta$ .

Ample numerical results are presented to validate our schemes and detailed comparisons are made with existing schemes to show their efficiency. Although we have only considered ground state solutions of BECs, the general approach presented in this paper can also be used to other minimization problems that can be reformulated as finding steady state solutions of imaginary time gradient flows.

### Acknowledgement

The authors would like to thank Professor Weizhu Bao for suggesting us to consider the two-component BECs and for stimulating discussions.

### References

- [1] A. Aftalion, Q. Du, Vortices in a rotating Bose-Einstein condensate: critical angular velocities and energy diagrams in the Thomas-Fermi regime, *Phys. Rev. A* 64 (6) (2001) 063603.
- [2] M.H. Anderson, J.R. Ensher, M.R. Matthews, C.E. Wieman, E.A. Cornell, Observation of Bose-Einstein condensation in a dilute atomic vapor, *Science* 269 (5221) (1995) 198–201.
- [3] X. Antoine, A. Levitt, Q. Tang, Efficient spectral computation of the stationary states of rotating Bose-Einstein condensates by the preconditioned nonlinear conjugate gradient method, *J. Comput. Phys.* 343 (2017) 92–109.
- [4] S. Ashhab, C. Lobo, External Josephson effect in Bose-Einstein condensates with a spin degree of freedom, *Phys. Rev. A* 66 (1) (2002) 013609.
- [5] W.Z. Bao, Ground states and dynamics of multicomponent Bose-Einstein condensates, *Multiscale Model. Simul.* 2 (2) (2004) 210–236.
- [6] W.Z. Bao, Y.Y. Cai, Ground states of two-component Bose-Einstein condensates with an internal atomic Josephson junction, *East Asian J. Appl. Math.* 1 (2011) 49–81.
- [7] W.Z. Bao, Y.Y. Cai, Mathematical models and numerical methods for spinor Bose-Einstein condensates, *Commun. Comput. Phys.* 24 (4) (2018) 899–965.
- [8] W.Z. Bao, Q. Du, Computing the ground state solution of Bose-Einstein condensates by a normalized gradient flow, *SIAM J. Sci. Comput.* 25 (5) (2004) 1674–1697.
- [9] W.Z. Bao, D. Jaksch, P.A. Markowich, Numerical solution of the Gross-Pitaevskii equation for Bose-Einstein condensation, *J. Comput. Phys.* 187 (1) (2003) 318–342.
- [10] W.Z. Bao, W.J. Tang, Ground-state solution of Bose-Einstein condensate by directly minimizing the energy functional, *J. Comput. Phys.* 187 (1) (2003) 230–254.
- [11] S.M. Chang, W.W. Lin, S.F. Shieh, Gauss-Seidel-type methods for energy states of a multi-component Bose-Einstein condensate, *J. Comput. Phys.* 202 (2005) 367–390.
- [12] Q. Cheng, J. Shen, Multiple scalar auxiliary variable (MSAV) approach and its application to the phase-field vesicle membrane model, *SIAM J. Sci. Comput.* 40 (6) (2018) A3982–A4006.
- [13] M.L. Chiofalo, S. Succi, M.P. Tosi, Ground state of trapped interacting Bose-Einstein condensates by an explicit imaginary-time algorithm, *Phys. Rev. E* 62 (2000) 7438–7444.



- [14] M. Edwards, K. Burnett, Numerical solution of the nonlinear Schrödinger equation for small samples of trapped neutral atoms, *Phys. Rev. A* 51 (1995) 138–1386.
- [15] B. Jackson, J.F. McCann, C.S. Adams, Vortex formation in dilute inhomogeneous Bose-Einstein condensates, *Phys. Rev. Lett.* 80 (1998) 3903–3906.
- [16] P. Muruganandam, S.K. Adhikari, Bose-Einstein condensation dynamics in three dimensions by the pseudospectral and finite-difference methods, *J. Phys. B* 36 (2003) 2501–2513.
- [17] X.R. Ruan, A normalized gradient flow method with attractive-repulsive splitting for computing ground states of Bose-Einstein condensates with higher-order interaction, *J. Comput. Phys.* 367 (2018) 374–390.
- [18] J. Shen, T. Tang, L.L. Wang, *Spectral Methods: Algorithms, Analysis and Applications*, Springer, Berlin, 2011.
- [19] J. Shen, J. Xu, Convergence and error analysis for the Scalar Auxiliary Variable (SAV) schemes to gradient flows, *SIAM J. Numer. Anal.* 56 (5) (2018) 2895–2912.
- [20] J. Shen, J. Xu, J. Yang, A new class of efficient and robust energy stable schemes for gradient flows, arXiv:1710.01331, 2017.
- [21] J. Shen, J. Xu, J. Yang, The scalar auxiliary variable (SAV) approach for gradient fluids, *J. Comput. Phys.* 353 (2018) 407–416.
- [22] J. Williams, R. Walsler, J. Cooper, E. Cornell, M. Holland, Nonlinear Josephson-type oscillations of a driven, two-component Bose-Einstein condensate, *Phys. Rev. A* 59 (1) (1999) R31.
- [23] X.W. Wu, Z.W. Wen, W.Z. Bao, A regularized Newton method for computing ground states of Bose-Einstein condensates, *J. Sci. Comput.* 73 (2017) 303–329.